

Cite this: *Nanoscale*, 2019, **11**, 2126

Received 13th October 2018,
Accepted 2nd January 2019

DOI: 10.1039/c8nr08294d

rsc.li/nanoscale

A sensitive and selective electroanalysis strategy for histidine using the wettable well electrodes modified with graphene quantum dot-scaffolded melamine and copper nanocomposites†

Yue Hua, Shuai Li, Yuanyuan Cai, Huan Liu, Yuqi Wan, Mengyuan Yin, Fengxiang Wang and Hua Wang *

A wettable well was fabricated on an electrode, which was further modified with carbon quantum dot-scaffolded nanocomposites of melamine and copper for probing histidine through a unique displacement reaction route. The developed electrode with wettable well enables the condensing enrichment of analytes from the sample droplets, improving the electroanalytical sensitivity.

L-Histidine (His) plays a crucial role in biological systems, for example, in the control of metal transportation¹ as His can strongly bind with some metal ions such as Cu²⁺ ions.^{2,3} Also, it can serve as a vital neurotransmitter or a neuromodulator in the mammalian central nervous system.⁴ Very high His levels may cause stress and psychological disorders such as anxiety, schizophrenia, and thrombotic disorders, whereas very low His levels may induce some diseases such as rheumatoid arthritis, nerve deafness, liver cirrhosis, and pulmonary disease.^{5,6} Moreover, the non-invasive analysis of His as the metabolites in human urine is preferred, since it may have higher concentration in urine than in blood.⁵ In particular, the urinary indicator of His is of clinical importance for monitoring human health, especially some serious diseases like metabolism disorders and “histidinemia”.^{5–7}

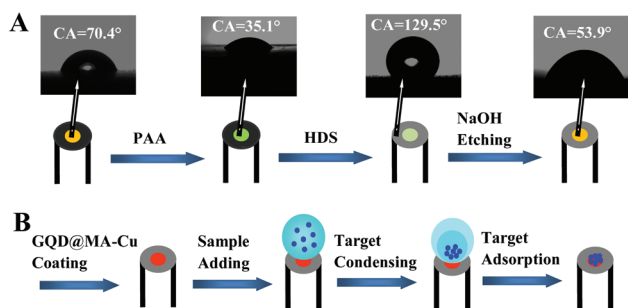
Over the past decades, a variety of analytical techniques have been applied for probing His in human body fluids and metabolites such as urine, with the help of high-performance liquid chromatography,^{8,9} capillary electrophoresis,^{10,11} fluorimetry,⁷ spectrophotometry,¹² and colorimetry.⁵ However, these

methods may involve either the utilization of bulky and expensive facilities or the tedious operation and complicated sample pre-treatment procedures.¹³ Alternatively, the electrochemical analysis methods with outstanding merits such as high sensitivity, easy operability, and portability of devices have been applied for the determination of His in recent years.^{13,14} For example, Liang *et al.* have reported the electrochemical detection of His based on the structure-switching DNAzymes and gold-graphene composites.¹⁴ Since most of the target metabolites may have considerably low levels in urine at the early stages of many diseases, the enrichment of the targets (*i.e.*, His) in the samples is highly desired prior to their detection. As an efficient route, the design of sensing platforms with super-hydrophobic surfaces, which elsewhere are usually applied for the anti-fouling, oil–water separation, and self-cleaning,^{15,16} have recently been employed to achieve the enrichment of some biomarkers from the samples.¹⁷ For example, Wang *et al.* developed a sensitive sensing platform by spotting wells onto the super-hydrophobic substrates for the improved enrichment and detection of nucleic acids. Due to this, the contact area of a sample droplet on the superhydrophobic surface can be favourably minimized, which is known as the “wettability”.^{18,19} The wettable testing area can allow the targets to be condensed from the droplet to provide improved analytical sensitivity.¹⁷

In this study, a wettable well was fabricated for the first time on a gold electrode, which was further modified with graphene quantum dot (GQD)-scaffolded nanocomposites of melamine (MA) and copper (GQD@MA–Cu) for the electroanalysis of His through the output of solid-state CuCl electrochemistry. Scheme 1A illustrates the fabrication process of a wettable well electrode. Polyacrylic acid (PAA) was first spotted on the sensing area of the electrode to produce the testing dot, and was then patterned with hydrophobic hexadecyltrimethoxysilane. Furthermore, the PAA-coated testing dot was etched with NaOH to yield a hydrophilic well on the electrode. It was noted that the resulting interface of the electrode could display the various hydrophilic–hydrophobic properties, as revealed by the

Institute of Medicine and Materials Applied Technologies, College of Chemistry and Chemical Engineering, Qufu Normal University, Qufu City, Shandong Province 273165, P. R. China. E-mail: huawang@qfnu.edu.cn; http://wang.qfnu.edu.cn; Fax: +86 537 4456306; Tel: +86 537 4456306

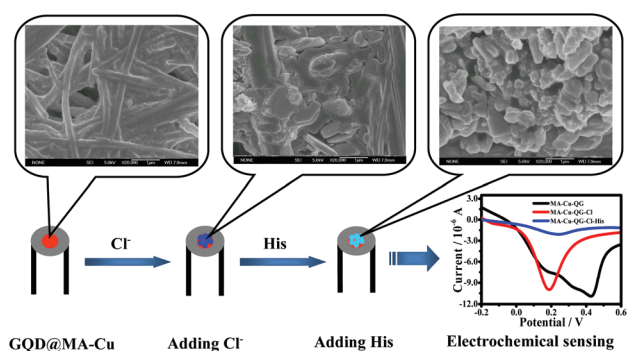
†Electronic supplementary information (ESI) available: The experimental section includes reagents and apparatus, synthesis of GQD@MA–Cu nanocomposites, fabrication of wettable well electrodes, and the electroanalysis of His in samples. Additional data are provided for the optimized detection conditions, XPS, UV spectra, conductivity characterization, electrochemical stability investigation, and comparison of analytical results among different analysis methods. See DOI: 10.1039/c8nr08294d



Scheme 1 Schematic illustration of (A) the fabrication process of a wettable well on the gold electrode including PAA spotting, HDS patterning, and NaOH etching, with the changing interface wettabilities manifested by CAs. (B) The enrichment procedure of the well electrode modified with GQD@MA–Cu nanocomposites for the condensation and adsorption of targets (Cl^- or His) from the sample droplet.

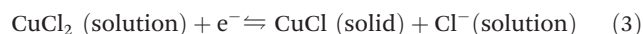
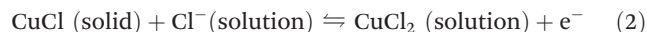
changing contact angles (CAs), of which the resulting well electrode could obtain the hydrophobic pattern (CA of 129.5°) and the hydrophilic well (CA of 53.9°) featuring the wettability.^{20–22} As illustrated in Scheme 1B, the targets (Cl^- or His) could be condensed from the sample droplets and adsorbed on the modified electrode, thus achieving greatly amplified electrochemical signals for more sensitive detections. Such a condensation-enrichment mechanism has also been described in literature.^{17,23} Accordingly, the sensing signals of the as-prepared electrodes with wettable GQD@MA–Cu wells could be thus amplified towards the sensitive His detection.

Scheme 2 manifests the sensing procedure of the wettable well electrode modified with the GQD@MA–Cu nanorods for the His electroanalysis, which is based on the displacement reaction route and solid-state CuCl electrochemistry. Herein, the GQD@MA–Cu nanocomposites were synthesized initially through the supramolecular self-assembly route using conductive graphene quantum dot (GQD) as the hollow scaffolds. GQD, as a newly-emerged carbon nanomaterial, consists of multi-layer graphene and different types of carbon allotropes with a high proportion of folded edges and surface defects,



Scheme 2 The electroanalytical sensing procedure of the GQD@MA–Cu-modified well electrode for Cl^- ions and then His with the electrochemical signal outputs, showing the corresponding SEM images of the resulting products (top).

which promise high sensitivity for sensing applications.^{24,25} Notably, the GQD scaffolds can interact with some polymers with conjugated structures such as MA through the strong non-covalent interactions such as the π - π stacking.²⁶ Furthermore, MA with three amino groups and three aromatic nitrogen atoms can be readily polymerized to act as the adsorbents for some metal ions including Cu^{2+} ions.^{27,28} Herein, it would serve as the reductant and the chelating agent for Cu^{2+} ions to yield the MA–Cu nanorods scaffolded by hollow GQD. The changing morphological features of the yielded products on the electrode were monitored by the scanning electron microscopy (SEM) images (top, Scheme 2). It was noted that the GQD@MA–Cu nanocomposites could display the well-defined nanorod-like structure. Once Cl^- ions were introduced, they could be broken down to produce large aggregated blocks, presumably due to the formation of CuCl precipitate through the interaction between Cl^- ions and Cu^+ ions in GQD@MA–Cu nanorods. More interestingly, block-type agglomerates could be largely obtained after the addition of His. In this case, His with three coordination sites (*i.e.*, amino nitrogen, imidazole, and carboxylate oxygen) can form stronger interactions with copper ions, which can form extremely stable complexes ($\log K = 18.1$).²⁹ Accordingly, an electrochemical process can take place on the electrodes modified with GQD@MA–Cu nanorods, involving the Cu redox chemistry as follows:



Herein, following a repetitive electrochemical process, Cu^+ in MA–Cu would first react with Cl^- ion in the solution to form the CuCl solid. Further, the CuCl solid would be electrochemically oxidized to yield CuCl_2 , which would be further reduced to CuCl in the reverse cathodic potential cycle. A displacement reaction between chloride and His would be triggered to induce the conversion of CuCl to the Cu–His complex, thus showing a rational decrease in the CuCl signals. Importantly, such a displacement reaction route may ensure improved His sensitivity, in contrast to most of the direct electrochemical responses to the analytes.^{13,14} Besides, the developed GQD@MA–Cu-modified well electrode can enable the His electroanalysis through the solid-state CuCl electrochemistry at a favorably low potential of about 0.20 V, which may aid in avoiding the interferences from other electroactive substances co-existing in the complicated biological media such as urine.

The GQD@MA–Cu products were analyzed by X-ray photoelectron spectroscopy (XPS) (Fig. S1, ESI†). One can observe that GQD@MA–Cu nanorods with Cl^- ions could include the key elements of C, N, O, Cl, and Cu (Fig. S1A–E†). In particular, Fig. S1F† reveals that the peak-fit profile of Cu $2p_{3/2}$ at 932.9 eV is composed of a series of satellites of Cu^+ and Cu^{2+} elements, in which, peak 1 belongs to Cu^+ and peak 2, 3, and 4

refer to the Cu^{2+} states.³⁰ The main conditions for the synthesis of GQD@MA-Cu nanocomposites were optimized; the most suitable MA-to-Cu ratio of 1/2 and GQD of 1.0 mg mL^{-1} was selected (Fig. S2, ESI†). Fig. S3A† exhibits the UV-Vis spectra of the as-prepared GQD@MA-Cu nanocomposites in comparison to the characteristic absorbances of Cu^{2+} ions, MA, and MA-Cu nanocomposites without GQD. One can see that the GQD@MA-Cu nanorods show no significant absorbance peak of copper ions (*i.e.*, around 300 nm), thus confirming the formation of GQD@MA-Cu nanocomposites by the supramolecular self-assembly route. Moreover, Fig. S3B† illustrates the comparison of the surface charge properties of the electrodes modified with GQD@MA-Cu and MA-Cu nanocomposites using $\text{K}_3[\text{Fe}(\text{CN})_6]$ as the electrochemical probe.³¹ As expected, the GQD@MA-Cu-modified well electrode could display much larger current responses than the one without GQD, indicating that GQD could boost the transfer of surface charges of the modified electrode. Also, the larger decrease in current caused by targeting His could be obtained by using the GQD@MA-Cu-modified well electrode. Moreover, Fig. S4A† shows that the peak currents of the developed well electrode could increase linearly with the scan rates ranging from 50 to 300 mV s^{-1} . The results validate that the CuCl oxidation reaction on the GQD@MA-Cu-modified well electrode is a surface-controlled process. In addition, the electrochemical sensing stability of the GQD@MA-Cu-modified well electrode was evaluated by the continuous CV scanning for 100 cycles (Fig. S4B†). It was found that the GQD@MA-Cu-modified well electrodes could maintain consistent CV responses, thus demonstrating a high sensing stability.

A comparison of linear sweep voltammetry (LSV) responses of Cl^- ions and His was carried out between the GQD@MA-Cu-modified electrodes with and without the well (Fig. 1A). One can observe that the developed well electrode could present much higher Cl^- response than the one without the well. More importantly, greater current response to His could be obtained for the well electrode, which is over two times larger than that of the one without the well. The data confirm that the GQD@MA-Cu-modified well electrodes can achieve drastically improved responses to His, demonstrating that the

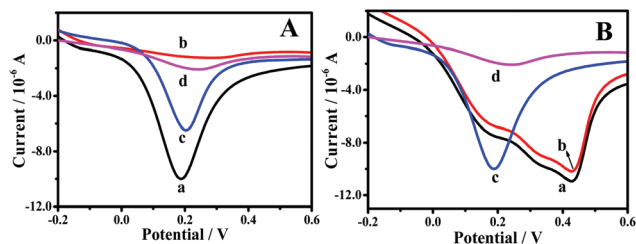


Fig. 1 (A) Comparison of the electrochemical responses between the GQD@MA-Cu-modified electrodes (a) with and (c) without a well when adding Cl^- ions, and then (b) and (d) adding His, respectively. (B) Comparison of characteristic electrochemical LSVs between GQD@MA-Cu-modified well electrodes in the (a) absence and (c) presence of Cl^- ions, with (b) and (d) the corresponding responses to His, respectively.

as-created wettable well could conduct the condensing enrichment for the targeted analytes (*i.e.*, His) from the sample droplet. Moreover, Fig. 1B reflects the comparison between the electrochemical His responses of the developed electrodes in the absence and presence of Cl^- ions. It was found that the introduction of Cl^- ions could endow the developed well electrode with a larger peak current of CuCl oxidation at a lower potential of about 0.20 V (curve c), in contrast to the one in absence of Cl^- ions showing a Cu oxidation peak at about 0.42 V (curve a). Herein, their current responses to His in the presence of Cl^- ions (curve d) could display a large difference at 0.20 V of the Cu/CuCl signal. In contrast, no significant change was observed at 0.42 V of copper oxidation in the absence of Cl^- ions (curve b), *i.e.*, a rational decrease in the solid-state CuCl signal could be specifically caused by His because of the stronger Cu-His interaction with a larger affinity constant ($\log K_{\text{His-Cu}} = 18.1$), thus achieving selective His electroanalysis. Also, the lower peak potential of CuCl electrochemistry (*i.e.*, 0.20 V) could be expected to circumvent the possible interferences from other electroactive backgrounds with the overlapped voltammetric signatures. In particular, His could induce a larger decrease in the CuCl current signals of the GQD@MA-Cu-modified well electrode (curve d), thus promising a highly selective and sensitive His electroanalysis.

Fig. 2 discloses the sensing selectivity of the GQD@MA-Cu-modified well electrode for the electroanalysis of His, in comparison to some other ions, small molecules, and amino acids possibly co-existing in urine. One can note that all of the tested analytes alone present negligible responses, except for cysteine (Cys) and lysine (Lys) (Fig. 2A), which display notice-

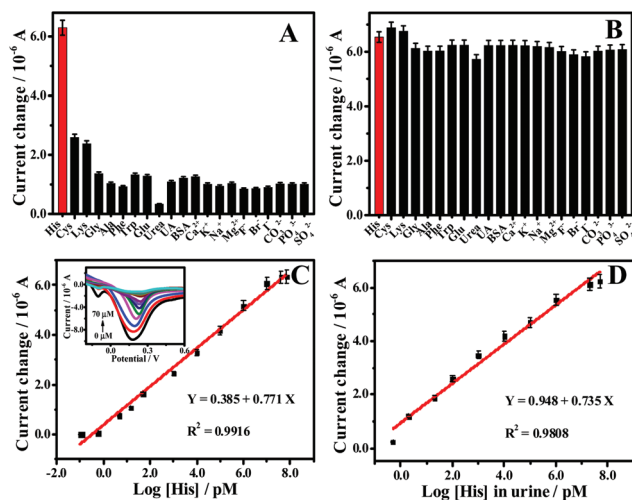


Fig. 2 Selective electrochemical responses of the GQD@MA-Cu-modified well electrode to (A) different interferents indicated alone, and (B) the interferents mixed separately with His with the same concentration ($50.0 \text{ }\mu\text{M}$). The calibration curves of the relationships between the current responses and different concentrations of His in (C) buffer (inset: the electrochemical LSV responses to His at different concentrations) and (D) spiked in urine samples.

able responses that are two-times lower than that of His at the same concentration. Furthermore, when these tested substances were separately mixed with His, no significant effect on the His responses was observed (Fig. 2B). Herein, the strong Cu–His interactions could induce the specific Cu–Cl displacement reactions to trigger the conversion of CuCl into the Cu–His complex, thereby leading to a rational decrease in the CuCl signals. Importantly, the displacement reaction endows the His electroanalysis with improved detection selectivity.

Therefore, the developed electroanalytical method can selectively probe His in the complicated biological samples such as urine. Moreover, the main conditions of the GQD@MA–Cu-modified well electrodes for the electroanalysis of His were investigated (Fig. S5, ESI†). The optimal probe dosage of 5.4 mg mL⁻¹ GQD@MA–Cu nanorods, pH 7.0, and 80 mM NaCl were chosen. Also, the detection reproducibility of the His electroanalysis method was evaluated using six GQD@MA–Cu-modified well electrodes, showing exceptionally high sensing reproducibility.

Under the optimized conditions, the developed GQD@MA–Cu-modified well electrodes were applied for the electroanalysis of different concentrations of His separately in buffer and urine samples (Fig. 2). It was discovered that the current responses of the developed electrodes would decrease with the increasing His concentrations (Fig. 2C, inset). A linear relationship was thus obtained for the electrochemical responses *versus* the log [His] ranging from 0.10 pM to 70.0 μM (Fig. 2C), with the limit of detection (LOD) of about 0.025 pM, estimated by the 3σ rule. Furthermore, the practical application of the developed electroanalytical method was performed by probing different concentrations of His spiked in urine samples (Fig. 2D). The results indicate that His in urine can be detected with the concentrations ranging from 0.50 pM to 50.0 μM, with the LOD of about 0.125 pM.

Additionally, the detection performances of the developed electroanalytical strategy were compared with those of other kinds of detection methods for His reported previously, with the analysis results summarized in Table S1.† One can note that the electroanalytical method developed by us can present better detection performance in terms of detection ranges and LODs.

Therefore, the developed electroanalytical strategy may promise improved clinical applications for the highly sensitive and selective sensing of His in various samples such as urine.

In summary, a wettable well electrode was successfully fabricated for the first time for the sensitive and selective electroanalysis of His in urine, based on the displacement reaction route and the solid-state CuCl electrochemistry. Herein, robust electrochemical probes of GQD@MA–Cu nanorods were initially synthesized by the supramolecular self-assembly route using conductive hollow GQD scaffolds. Compared to the traditional electroanalytical methods with copper nanomaterials, the developed GQD@MA–Cu-modified well electrodes could obtain a stable output of solid-state CuCl electrochemistry at a desirably low potential (0.20 V), which may avoid the possible

interferences from electroactive substances co-existing in the complicated biological media like urine. Moreover, the detection of His was realized through the specific and strong Cu–His interaction to trigger the displacement of Cl⁻ in CuCl to give the Cu–His complex. In contrast to most of the direct electrochemical responses to analytes, this displacement reaction route could achieve improved sensitivity. More importantly, the well created on the electrode can feature the wettability, which can conduct the condensing enrichment of analytes (*i.e.*, His) from the sample droplet, so as to achieve increased detection sensitivity. The developed electroanalytical strategy was subsequently applied for the fast evaluation of His in urine samples with sufficiently high sensitivity and selectivity, which are comparably better than those of the current detection methods for His. Therefore, the developed electroanalytical method with the portable sensing device may find field-deployable applications for probing the low-level His in various biological media (*i.e.*, blood and urine) for the early warning or diagnosis of serious diseases. In addition, the proposed fabrication protocol for constructing a wettable well on the electrode would open a new door towards the large-scale design of a variety of electrode arrays with the wettability feature for the condensing enrichment of analytes, which can promise high throughput and sensitive biological analysis.

Conflicts of interest

There are no conflicts to declare.

Acknowledgements

This study is supported by the National Natural Science Foundations of China (No. 21675099 and 21375075), the Taishan Scholar Foundation of Shandong Province, P. R. China, and Major Basic Research Program of Natural Science Foundation of Shandong Province, P. R. China (ZR2018ZC0129).

Notes and references

- 1 X. Zheng, T. Yao, Y. Zhu and S. Shi, *Biosens. Bioelectron.*, 2015, **66**, 103–108.
- 2 L. D. Pettit and J. L. M. Swash, *Cheminf.*, 1976, **7**, 588–594.
- 3 L. Zhou, S. Li, Y. Su, X. Yi, A. Zheng and F. Deng, *J. Phys. Chem. B*, 2013, **117**, 8954–8965.
- 4 Y. Hu, Q. Wang, C. Zheng, L. Wu, X. Hou and Y. Lv, *Anal. Chem.*, 2014, **86**, 842–848.
- 5 S. K. Sun, K. X. Tu and X. P. Yan, *Analyst*, 2012, **137**, 2124–2128.
- 6 S. Qiu, M. Miao, T. Wang, Z. Lin, L. Guo, B. Qiu and G. Chen, *Biosens. Bioelectron.*, 2013, **42**, 332–336.
- 7 J. T. Hou, K. Li, K. K. Yu, M. Y. Wu and X. Q. Yu, *Org. Biomol. Chem.*, 2013, **11**, 717–720.

- 8 N. Tateda, K. Matsuhisa, K. Hasebe and T. Miura, *Anal. Sci.*, 2001, **17**, 775–778.
- 9 S. Wadud, M. M. Or-Rashid and R. Onodera, *J. Chromatogr. B: Anal. Technol. Biomed. Life Sci.*, 2002, **767**, 369–374.
- 10 L. Zhou, N. Yan, H. Zhang, X. Zhou, Q. Pu and Z. Hu, *Talanta*, 2010, **82**, 72–77.
- 11 L.-Y. Zhang and M.-X. Sun, *J. Chromatogr. A*, 2004, **1040**, 133–140.
- 12 J. D. Swartz, C. P. Gulka, F. R. Haselton and D. W. Wright, *Langmuir*, 2011, **27**, 15330–15339.
- 13 L. D. Li, Z. B. Chen, H. T. Zhao and L. Guo, *Biosens. Bioelectron.*, 2011, **26**, 2781–2785.
- 14 J. Liang, Z. Chen, L. Guo and L. Li, *Chem. Commun.*, 2011, **47**, 5476–5478.
- 15 W. Zhang, Z. Shi, F. Zhang, X. Liu, J. Jin and L. Jiang, *Adv. Mater.*, 2013, **25**, 2071–2076.
- 16 B. Su, S. Wang, Y. Wu, X. Chen, Y. Song and L. Jiang, *Adv. Mater.*, 2012, **24**, 2780–2785.
- 17 L. P. Xu, Y. Chen, G. Yang, W. Shi, B. Dai, G. Li, Y. Cao, Y. Wen, X. Zhang and S. Wang, *Adv. Mater.*, 2015, **27**, 6878–6884.
- 18 X. Feng, J. Zhai and L. Jiang, *Angew. Chem., Int. Ed.*, 2005, **44**, 5115–5118.
- 19 S. Wang, X. Feng, J. Yao and L. Jiang, *Angew. Chem., Int. Ed.*, 2006, **45**, 1264–1267.
- 20 L. Feng, M. Liu, H. Liu, C. Fan, Y. Cai, L. Chen, M. Zhao, S. Chu and H. Wang, *ACS Appl. Mater. Interfaces*, 2018, **10**, 23647–23656.
- 21 S. Li, M. Dong, R. Li, L. Zhang, Y. Qiao, Y. Jiang, W. Qi and H. Wang, *Nanoscale*, 2015, **7**, 18453–18458.
- 22 S. Li, R. Li, M. Dong, L. Zhang, Y. Jiang, L. Chen, W. Qi and H. Wang, *Sens. Actuators, B*, 2016, **222**, 198–204.
- 23 M. Liu, L. Feng, X. Zhang, Y. Hua, Y. Wan, C. Fan, X. Lv and H. Wang, *ACS Appl. Mater. Interfaces*, 2018, **10**, 32038–32046.
- 24 E. P. Randviir, D. A. Brownson, M. Gomez-Mingot, D. K. Kampouris, J. Iniesta and C. E. Banks, *Nanoscale*, 2012, **4**, 6470–6480.
- 25 M. Dong, C. Liu, S. Li, R. Li, Y. Qiao, L. Zhang, W. Wei, W. Qi and H. Wang, *Sens. Actuators, B*, 2016, **232**, 234–242.
- 26 R. Shen, W. Zhang, Y. Yuan, G. He and H. Chen, *J. Appl. Electrochem.*, 2015, **45**, 343–352.
- 27 M. X. Tan, Y. N. Sum, J. Y. Ying and Y. Zhang, *Energy Environ. Sci.*, 2013, **6**, 3254–3259.
- 28 Y. Zhao, L. Xu, S. Li, Q. Chen, D. Yang, L. Chen and H. Wang, *Analyst*, 2015, **140**, 1832–1836.
- 29 J. F. Folmer-Andersen, V. M. Lynch and E. V. Anslyn, *Chemistry*, 2005, **11**, 5319–5326.
- 30 M. Yin, C. K. Wu, Y. Lou, C. Burda, J. T. Koberstein, Y. Zhu and S. O'Brien, *J. Am. Chem. Soc.*, 2010, **36**, 9506–9511.
- 31 Z. O. Ameer and M. M. Husein, *Sep. Sci. Technol.*, 2013, **48**, 681–689.